

低解析車牌影像之辨識

研究生：廖昱嘉

指導教授：陳玲慧 博士

國立交通大學多媒體工程研究所碩士班

摘要

近年來，雖然有許多關於車牌影像辨識的相關研究，但是卻鮮少有研究使用低解析的車牌影像作為輸入來進行辨識。因此，本論文將著墨在使用低解析度的車牌影像來進行辨識。這個方法可以處理極小的車牌影像，而且僅需單張車牌影像就可以進行處理。首先，針對單張影像，以人工方式將車牌區域截取出來作為輸入，並進行連字符號的偵測以及定位車牌字母。其次，根據上個步驟所得之結果，使用單一字母進行樣版比對(template matching)，並挑選出適合的候選字母。最後，將單一字母樣版擴充至多重字母樣版來進行比對，逐步篩選並簡化辨識的結果。實驗結果顯示該方法對於低解析度的車牌影像具有相當的辨識率，且其結果也可有效應用在進行犯罪調查時，用以縮減嫌疑車輛的搜尋範圍。

Recognition of Low-resolution Vehicle License Plate Images

Student : Yu-Chia Liao

Advisor : Dr. Ling-Hwei Chen

Institute of Multimedia Engineering

College of Computer Science

National Chiao Tung University

ABSTRACT

Although there are lots of studies about recognizing vehicle license plate (VLP) images in recent years, the recognitions of low resolution VLP image are still deficient. The proposed method focuses on the recognitions of low-resolution VLP image. This method can treat VLP images with pretty small size, and only a single VLP image is need. First, the hyphen detection and character position estimation will be applied on a manually cropped VLP image which is seriously blurred. Then, a single-character template matching will be performed based on the estimated positions. Finally, the refinement of recognition results from the single-character template matching will be conducted via expanding a single-character template to a

multiple-character template. Experiment results show that the proposed method is quite efficient to recognize VLP images with low resolution. The results are helpful for locating a suspect vehicle on a low-resolution image in the field of crime investigation.



誌 謝

能夠完成這篇論文，首先要感謝指導教授陳玲慧博士無私的指導與帶領。在攻讀交大碩士的這兩年中，陳老師親切的指導與關鍵的提醒總是讓我獲益匪淺，讓我除了學習到研究的態度與方法外，也學不少待人處事與進退應對的道理。此外，感謝李建興教授與陳佑冠教授於口試中給予的建議與指導，使我能夠發現自己研究的缺失與不足，使得整篇論文更佳完善。

其次，在碩士生活中，實驗室的夥伴們在身心上也提供了我不少支援。感謝實驗室學長姐惠龍、文超、俊旻、占和、盈如、芳如和懷三對我的指導與建議，無論是課業上，或者是生活上，都非常感謝他們讓我備感溫馨的提醒與關懷。感謝實驗室學弟妹文豪、佩庭與婉甄，很高興能在碩二時能有你們的陪伴與關心。更要感謝同窗的志錡與明昌，在那段一起修課與研究的日子中，感謝你們的陪伴和照應，這段充實且難以忘懷的時光，也是我能夠繼續走下去的動力。

此外，同樣感謝關心我的朋友們，感謝他們對我的鼓勵與關懷。感謝大學時期幾位要好的同窗，每隔半年的相聚總是讓我歡笑不已，互相的關懷與勉勵更是讓我更加窩心。最後，感謝我的家人，感謝爸爸、媽媽、奶奶、姑姑和哥哥，一直以來，總是以自己的方式給予我支持與鼓勵，讓我這一路上不會有太多負擔與壓力，也讓我得以在疲憊時有喘息的時光與空間，使我能在休息過後重新出發，迎接待克服的難關與挑戰。謹以此篇論文呈獻給所有關心與協助我的人，在下感激不盡。

CONTENTS

ABSTRACT (IN CHINESE).....	i
ABSTRACT (IN ENGLISH).....	ii
ACKNOWLEDGE (IN CHINESE).....	iv
CONTENTS.....	v
LIST OF FIGURES	vii
LIST OF TABLES.....	viii
CHAPTER 1 INTRODUCTION	1
1.1 Motivation.....	1
1.2 Related Works.....	2
1.3 Organization of the Thesis	8
CHAPTER 2 THE PROPOSED METHOD	9
2.1 Hyphen Detection	13
2.2 Character Position Estimation.....	16
2.3 Template Normalization	17
2.3.1 Size Normalization	18
2.3.2 Intensity Normalization	20
2.4 Similarity Measurement.....	21
2.5 Candidate Character Set Estimation	23
2.6 Recognition Based on Multiple-Character Templates	24
CHAPTER 3 EXPERIMENTAL RESULTS	28

3.1 Experiments of Resizing	28
3.2 Experiments of Proposed Method.....	33
CHAPTER 4 CONCLUSIONS AND FUTURE WORK.....	38
REFERENCES	40



LIST OF FIGURES

Fig. 1	An example of VLP region cropping from low resolution image.	9
Fig. 2	The block diagram of the proposed method.	11
Fig. 3	The flow chart of character segmentation.	11
Fig. 4	The flow chart of single-character template matching.	12
Fig. 5	The flow chart of multiple-character template matching.	12
Fig. 6	Character templates from high-resolution images.	18
Fig. 7	The result of similarity measurement via L1 distance.	22
Fig. 8	The result of similarity measurement via correlation coefficient.	22
Fig. 9	An example of candidate character set estimation with the candidate characters associated for each character position.	24
Fig. 10	The hierarchical structure of multiple-character template.	25
Fig. 11	The top survived 5 two-character templates after applying two-character template matching for positions 1 and 2.	27
Fig. 12	The top survived 5 two-character templates after applying two-character template matching for positions 4 and 5.	27
Fig. 13	Recognition result of VLP "5880-JJ", (a) The low-resolution VLP image. (b) The cropped VLP image. (c) The top 5 ranks of recognition result: "5880-JJ", "5880-J3", "5980-JJ", "5898-JJ" and "5380-JJ".	35
Fig. 14	Recognition result of VLP "8H-1879", (a) The low-resolution VLP image. (b) The cropped VLP image. (c) The top 5 ranks of recognition result: "BH-1879", "8H-1879", "RH-1879", "BN-1879" and "BR-1879".	35
Fig. 15	The images of VLP "2536-TX" and "M0-1860".	37

LIST OF TABLES

Table 1	An example of the process of hyphen detection.....	16
Table 2	The recognition results of using Gaussian, mean average and bicubic for resizing.....	29
Table 3	The recognition results of using different resizing methods on VLP “8H-1879”.....	30
Table 4	The recognition results of using different resizing methods on VLP “7885-TW”.....	31
Table 5	The recognition results using L1 distance and correlation coefficient for 15 VLP images.....	32
Table 6	The recognition results using different overlap ranges for 15 VLP images. .	33
Table 7	Recognition results of 50 cropped VLP images.	36
Table 8	The recognition result of the proposed method.	36

CHAPTER 1

INTRODUCTION

1.1 Motivation

With the advance of science and technology in recent years, it is more common to see video surveillance systems in cities to monitor the traffic movements and the potential criminal activities on public routes. Besides, thanks to the popularity of camera phone, people may have their own chance to capture a photo of the suspect vehicle when seeing an untoward incident on the road, such as car accidents, or even the vehicles of criminals.

Unfortunately, both kinds of video clips or images have the same problem. For video surveillance systems, the resolutions of videos are usually low because the cost of running a surveillance system is really expensive. Also, the camcorders are set outside, so the quality of images are often blurred. For camera phones, people usually have a distance from the suspect vehicle when taking photos from their camera phone, so the quality and resolution are poor.

Most of the vehicle license plate (VLP) recognition systems with high accuracy are designed for automatic toll booth or parking lot management, there are not

suitable for incoming images seriously blurred. Because of the poor plate resolution of an image, it becomes a big challenge to recognize characters on the VLP of a suspect vehicle from a low resolution image.

Although many forensics-related research institutes around the world have devoted a great deal of effort to deal with this issue, a systematic way that can either solve the problem or show that it is not solvable is still deficient. Therefore, we attempt to propose a VLP recognition method that is able to solve images with poor resolution.

1.2 Related Works

Numbers of research have been proposed to recognize characters on VLP images in the past decades. According to the survey presented by Anagnostopoulos et al. [1], the license plate recognition algorithms are generally composed of three conventional steps as the following:

- A. license plate detection [2] [3],
- B. character segmentation [4] [5],
- C. character recognition [6-13].

As to the license plate detection step, no matter in the field of binary, gray-scale or color image processing, lots of algorithms are designed to extract the VLP region

in the input image or video clip, such as histogram processing, spatial measurements and morphology. Bai et al. [2] presented a hybrid license plate algorithm based on edge statistics and morphology for the monitoring the highway ticketing systems. Wu et al. [3] proposed a novel method to extract license plate from the surveillance video which was shot at lower resolution (320×240) as well as degraded by video compression. Morphological operations of bottom-hat and morphology gradient are utilized to detect the license plate candidates, and effective schemes are applied to select the correct one.

On the issue of character segmentation, the horizontal and vertical projections are widely used to segment each character from the detected VLP region. Zhang et al. [4] proposed segmentation using Hough transformation and the prior knowledge in horizontal and vertical segmentation based on the projection analysis. The research presented by Nomura et al. [5] , which was completely dedicated to the task of character segmentation, describes a mathematical morphology-based adaptive approach for degraded plate images.

For the character recognition step, numerous methods try to use statistical classifiers [6-7] , computational intelligence architectures [8] , and conventional template-matching approaches [9-13] to solve the issue. Llorens et al. [6] presented a system for finding license plate based on the analysis of connected components of

four different binarizations of the image, and the system recognizes characters via means of Hidden Markov Models. Kim et al. [7] presented a system that implements SVMs with a good recognition result for Korean plates. Four SVM-based character recognizers were applied to recognize upper characters, upper numerals, lower characters, and lower numerals on the plate. Chang et al. [8] proposed an automatic license plate recognition system with two main modules: a license plate locating module and a license number identification module. The latter conceptualized in terms of neural subjects aims to identify the number present in a license plate. It consists of the topological feature sorting and the template test via self-organizing character recognition, which was based on Kohonen's self-organizing neural network. Huang et al. [9] and Wu et al. [10] both presented an automatic system to recognize the license number of the license type of their own country in the acquired image via a template matching technique. Bellas et al. [11] presented an automation methodology on an FPGA-based license plate recognition system via pixel-wise comparison between the sub-region of license plate image and preloaded image of a character, as well as comparison of the horizontal projection of each column and the vertical projection of each row of the characters. Barroso et al. [12] proposed a plate reading system, which was based in the critical points method and used template matching to disambiguate between characters which were classified in the same class. Comelli et

al. [13] presented a system for the recognition of car license plates. The process of character recognition extracted some feature points and used template matching operators to get a robust solution under multiple acquisition conditions. All of the above-mentioned researches are conventional pattern recognition-based approaches.

The authors in [1] mentioned that although several studies can get a successful plate localization when the vertical resolution (height) of VLP is small, the poor plate resolution does not allow the reliable extraction of characters on the plate. They also mentioned that most of recognition errors in the license plate recognition systems are not due to missing recognition power but to the segmentation errors, and poor resolution usually degrade the segmentation performance.

In other words, the accuracy of recognition depends on the result of character segmentation for the conventional pattern recognition-based type approach. Because we will deal with seriously blurred images which are caused via the affection of low resolution, the boundary of any two neighboring characters on the VLP is hard to detect (even not exist), we cannot use segmentation methods mentioned above to get a good result.

In recent years, super-resolution-based approach has been proposed as an another choice to solve low-resolution VLP recognition. Unlike traditional pattern recognition-based approaches, a super-resolution-based approach will try to improve

the quality of images at first then perform recognition later. The high-resolution image is usually obtained by fusing the information derived from multiple, subpixel shifted, and noisy low-resolution images. Lin et al. [14] proposed a non-uniform interpolation method to reconstruct license plate image from a series of low resolution vehicle license plate images. Suresh et al. [15] proposed a novel method that the image to be superresolved is modeled as Markov random field and estimated from the observations by a graduated nonconvexity optimization procedure, and a discontinuity adaptive regularizer is used to preserve the edges in the reconstructed number plate for improved readability. Rajaram et al. [16] presented a novel machine-learning-based framework for zooming and recognizing images of digits obtained from vehicle registration plates, which have been blurred using an unknown kernel. They modeled the image as an undirected graphical model over image patches in which the compatibility functions are represented as nonparametric kernel densities. Tian et al. [17] proposed a new algorithm to perform single-frame image super-resolution (SR) of vehicle license plate using soft learning prior. This method integrated image SR with optical character recognition to perform VLP SR. The soft learning prior estimated the importance of different learning samples, and integrates this information into high-resolution reconstruction of the license plate.

However, for the super-resolution-based approach, the current trend is to

super-resolve multiple low-resolution images to a high resolution image, the different perspective effect of each image will cause the registration more difficult. Also, these approaches may “modify” the content of the target VLP image, this is unacceptable in the forensics-related fields.

Some methods for low-resolution VLP recognition were proposed in recent years. Chen et al. [18] presented a novel hybrid method for extracting license plates and recognizing characters from low-quality videos using morphological operations and AdaBoost algorithm. Mistubishi Heavy Industries, Ltd. (MHI) [19] developed three technologies based on the conventional license plate recognition system using still images from low-resolution camera. These technologies improve image quality, process plural images of a single vehicle, and utilize a reference database. Hsieh et al. [20] presented a system which only uses one single VLP image without character segmentation to perform character recognition in blurred VLP images. They used single character template matching to estimate the potential positions via finding the local minima of the minimum similarity curve, which was obtained from the all similarity values at corresponding position of each character template.

However, despite an low quality input video is used in the research of [18] , the boundary of any two neighboring characters on the VLP still could be detected. This method may not work when the images are too blurred or the plate region are too

small. The method proposed by MHI [19] used multiple VLP image, so the input resource was limited to video clips, not a single VLP image. The method presented by Hsieh [20] may consider all characters as candidates when some character positions cannot be detected, or wrong character positions are found, this would lead to the wrong recognition result.

The proposed method will focus on the recognition of a single low-resolution VLP image. First, the hyphen detection and character position estimation will be provided on a manually cropped VLP image. Then, the single-character template matching will be performed based on the estimated positions. Finally, the refinement of recognition results from single-character template matching will be conducted via expanding the single-character template to multiple-character template.

1.3 Organization of the Thesis

The thesis is organized as follows. In Chapter 1, the motivation and related works are introduced. The proposed template matching method of VLP recognition is introduced in next chapter. In Chapter 3, experimental results will be given. Finally, conclusions and future work will be depicted in Chapter 4.

CHAPTER 2

THE PROPOSED METHOD

In this chapter, we describe the proposed recognition method for low-resolution VLP images. First, we crop the license plate region from the image with the suspect vehicle manually as our input. Fig. 1 is an example of cropping VLP image from a low-resolution image. Our approach focus on low-resolution VLP images in Taiwan which cannot be read by human directly.



Fig. 1 An example of VLP region cropping from low resolution image.

Before describing the proposed method, we first introduce the VLP of a light vehicle in Taiwan. In Taiwan, characters in a VLP can be Latin alphabets (A to Z), Arabic numerals (0 to 9) and a hyphen or dash (-). The characteristic of the VLP of a light vehicle is showed as follows. There are six characters and one hyphen on the VLP. The characters are separated into two regions by a hyphen, the character region

and the digit region; the former is composed of two characters, which can be alphabets or digits. The latter is composed of four characters, which only can be digits. The size of each character is 45 mm×90 mm, the size of hyphen is 10 mm×90 mm, and the width of the white space between two neighboring characters or between one character and the hyphen is 5 mm.

The block diagram of the proposed method is shown in Fig. 2. The proposed method is composed of three steps, which are character segmentation, single-character template matching and multiple-character template matching. Character segmentation is proposed at first, and Fig. 3 shows the flow chart of character segmentation. In this stage, hyphen detection and character position estimation are applied on the cropped VLP image. Next, single-character template matching is proposed. Fig. 4 is the flow chart of single-character template matching. The extracted information from cropped VLP image is used to implement template normalization and similarity measurement with high-resolution single-character templates, then the candidate character set estimation is performed to generate the single-character candidate lists. Finally, we extend single-character template matching to multiple-character template matching. Fig. 5 shows the flow chart of multiple-character template matching. The extending process starts from templates concatenation, which generates high-resolution multiple-character templates. Those templates then are used to perform the same

process as those in single-character template matching, these include template normalization, similarity measurement and character candidate set estimation. The whole process will end when the six-character candidates are generated.

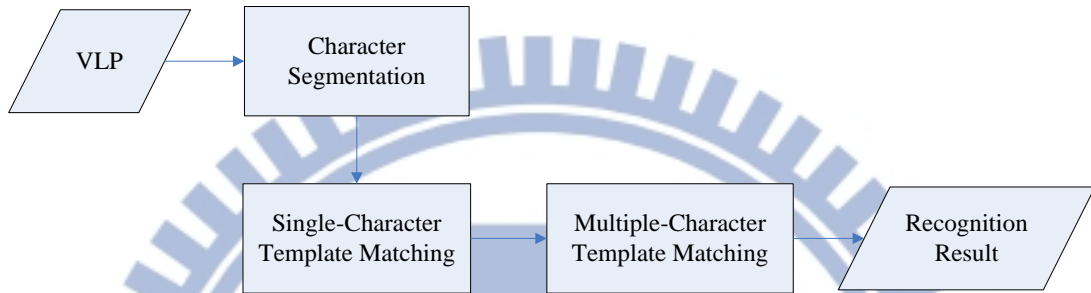


Fig. 2 The block diagram of the proposed method.

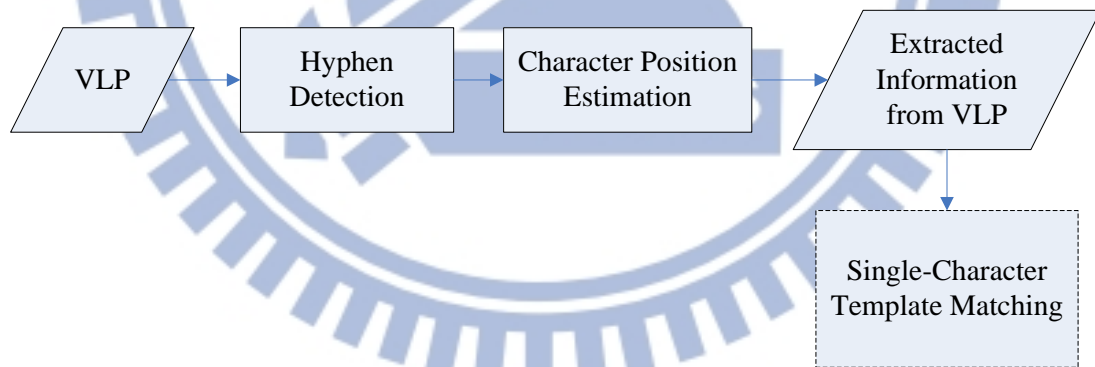


Fig. 3 The flow chart of character segmentation.

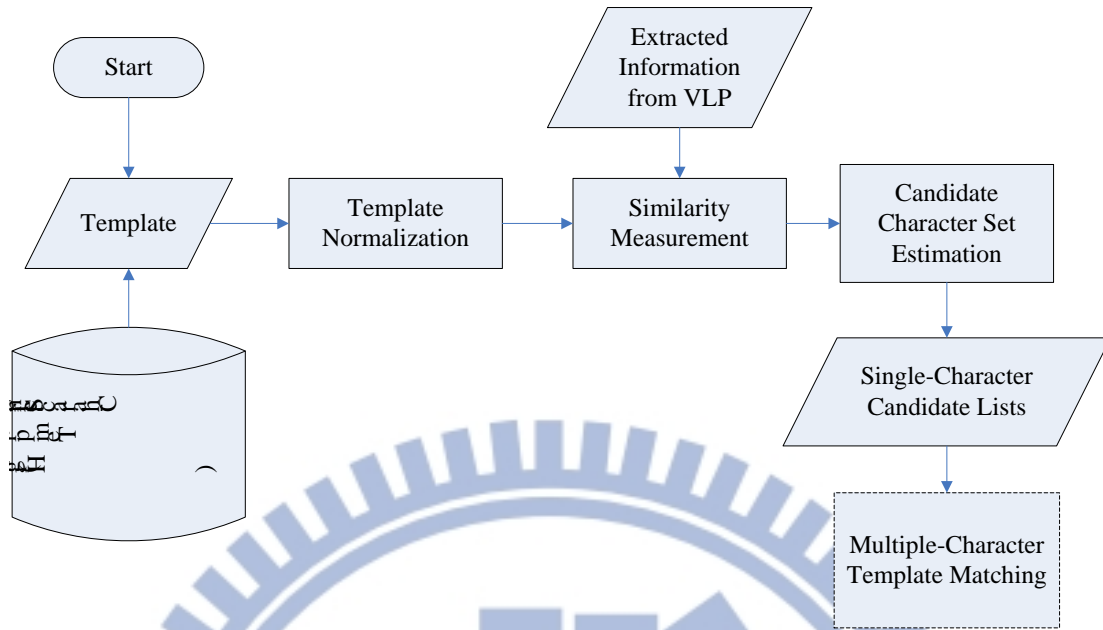


Fig. 4 The flow chart of single-character template matching.

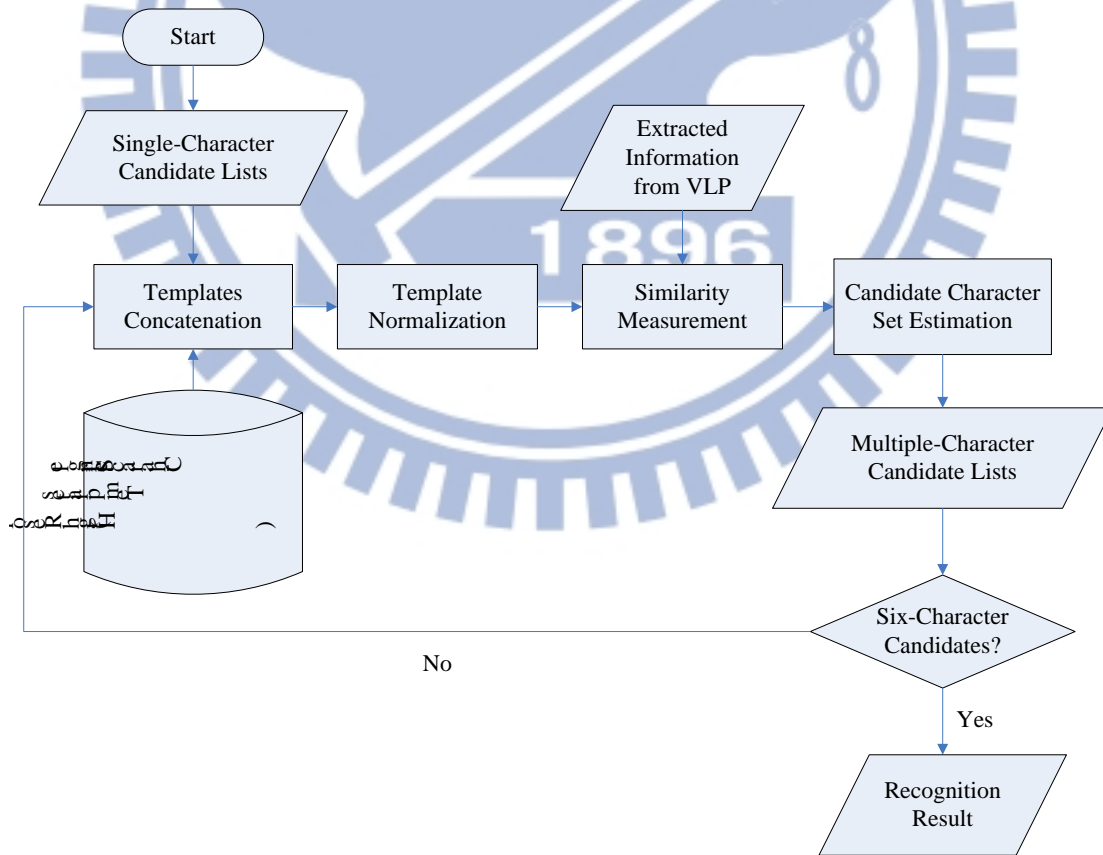


Fig. 5 The flow chart of multiple-character template matching.

2.1 Hyphen Detection

Note that the character region and the digit region of VLP in Taiwan are separated by a hyphen, this means that if we can find the position of hyphen, we can reduce most of the character candidates, which are the alphabets but stand in the digit region.

According to the characteristics of VLPs in Taiwan, we already know the real size of each character and hyphen. Considering the white space between the neighboring characters in, the width of hyphen is three tenths of the width of a single character. Defining ROI as the possible x -locations of hyphen in the VLP image, the hyphen should sit between the 2nd and the 3rd or the 4th and the 5th characters, so there are two possible ROIs.

First, define the cropped VLP image as LP , the resolution of VLP as $H_{LP} \times W_{LP}$. The width of the hyphen W_{hyphen} can be calculated by (1). The ratio of width to height of a single character is 1:2, and the ratio of the width of a hyphen to the width of a single character is 3:10.

$$W_{hyphen} = H_{LP} \times \frac{1}{2} \times \frac{3}{10}. \quad (1)$$

The width of a single character on the VLP W_{SC} can be calculated by (2).

$$W_{SC} = \frac{W_{LP} - W_{hyphen}}{6}. \quad (2)$$

Then we can determine initial estimation of two possible locations of hyphen P_L and P_R by following equations:

$$\begin{aligned} P_L &= W_{SC} \times 2, \\ P_R &= W_{SC} \times 4. \end{aligned} \quad (3)$$

Based on the initial possible position of hyphen, the hyphen detection is conducted, the ranges of ROIs are set to $[P_L - W_{hyphen}, P_L + W_{hyphen}]$ and $[P_R - W_{hyphen}, P_R + W_{hyphen}]$. Next, we analyze the vertical projection at ROIs, which means the summation of intensity values in each column of ROIs, and the intensity value of the center point in each column of ROIs.

For the vertical projection at ROIs, the higher the value of the vertical projection at a certain point is, the greater the possibility of hyphen at that point is. For the intensity value in each column of ROIs, according to the pattern of hyphen, in the vertical direction, the top region and the bottom region are white, and the middle region is black. We design an algorithm to do hyphen detection based on these features.

In the estimated ranges of ROIs, the vertical projection analysis is used at first, the result of vertical projection is ordered from high to low, and then the following process is performed in this order. Next, to reduce the affection of aliasing caused by the poor plate resolution, we rescale the intensity values from $0 \sim 255$ to $0 \sim 25$, and

the analysis of intensity values in each column is performed. If we find that the lowest intensity value is in the middle part of a column, the position of hyphen is detected.


Table 1 shows an example of the process of hyphen detection mentioned above.

According to the initial estimation, W_{hyphen} is 1, P_L and P_R are 6 and 12, so the corresponding ranges of ROIs are [5, 7] and [11, 13], respectively. In Table 1 (a), the first row shows the ROIs with centers at P_L and P_R . The second row shows the intensity of each point at each column, the third row shows the vertical projection value at each candidate position, and the last row shows the ordering of vertical projection (VP) values from high to low. Table 1 (b) shows the normalized intensity values, and the middle point of column 12 with the smallest vertical projection value and being a local minimum. The result shows that the position of hyphen is confirmed, and it is located between the 4th and 5th characters.

Table 1 An example of the process of hyphen detection.

(a)

5 8 8 0 - J J



ROI	5	6	7	~	11	12	13
Intensity value	93	82	71		80	110	118
	75	81	77		75	113	126
	83	77	66	~	87	103	126
	67	91	95		90	115	104
	95	93	81		105	118	67
VP	413	424	390	~	437	559	541
Order	5	4	6	~	3	1	2

(b)

ROI	5	6	7	~	11	12	13
Norm. intensity value	9	8	7		8	11	11
	7	8	7		7	11	12
	8	7	6		8	<u>10</u>	12
	6	9	9	~	9	11	10
	9	9	8		10	11	6
Order	5	4	6	~	3	1	2

2.2 Character Position Estimation

In the stage of hyphen detection, we have already estimated the width of a single character W_{SC} , the width of the hyphen W_{hyphen} , and the position of the hyphen, so we can get an initial position of each character.

Let i represents the index of the i -th character, and Pos_i responds to the position of the character. According to the position of hyphen, if the hyphen is in

between the 2nd and 3rd characters, the initial position of each character is set to:

$$\begin{cases} Pos_i = i \times W_{SC}, i = 0, 1 \\ Pos_i = i \times W_{SC} + W_{hyphen}, i = 2 \sim 5. \end{cases} \quad (4)$$

Otherwise, the initial position of each character is set to:

$$\begin{cases} Pos_i = i \times W_{SC}, i = 0 \sim 3 \\ Pos_i = i \times W_{SC} + W_{hyphen}, i = 4, 5. \end{cases} \quad (5)$$

The candidate character set estimation will be performed based on these locations.

2.3 Template Normalization

Because the proposed method is based on the use of template matching, we have to collect images of every possible character as our input templates. These character templates are obtained from high-resolution VLP images directly, and the initial normalization of size and intensity are required to make these templates have the same size and the same intensity level before we use them as templates. Fig. 6 shows the character templates from high-resolution images.

To apply template matching, the difference of size and intensity between each template and the target VLP image should be concerned, so the normalization work is performed at first to compensate this difference.



Fig. 6 Character templates from high-resolution images.

2.3.1 Size Normalization

The size of templates should be normalized to fit the size of VLP before we perform matching, so we have to determine the normalization size, and perform a method of resizing to get suitable templates.

The size of normalized template is determined by the following equations:

$$\begin{aligned} H_{LT} &= H_{LP}, \\ W_{LT} &= \frac{W_{HT}}{H_{HT}} \times H_{LT}, \end{aligned} \quad (6)$$

where LT is the normalized template, and HT is the original high-resolution template; H and W are the height and the width respectively. The purpose is to make the height of normalized templates the same as the height of LP .

For the resizing, we have testified several methods, these methods we have tried

are as follows:

- A. Bilinear interpolation,
- B. Bicubic interpolation,
- C. Mask of Gaussian,
- D. Mask of mean average,
- E. Mask of Gaussian with overlap,
- F. Mask of mean average with overlap.

Both A and B are the traditional methods to perform resizing, they generate new data point via interpolating the original data points on the two dimensional regular grid. The key idea of bilinear interpolation is to perform linear interpolation first in one direction, and then again in the other direction. Although each step is linear in the sampled values and in the position, the interpolation as a whole is not linear but rather quadratic in the sample location. In contrast to bilinear interpolation, which only takes 4 pixels (2x2) into account, bicubic interpolation considers 16 pixels (4x4). Images resampled with bicubic interpolation are smoother and have fewer interpolation artifacts.

The main idea of C and D are the same, it uses the spatial filter to shrink the origin image into a small size. The size of mask M is calculated as follows:

$$\begin{aligned}
H_M &= \frac{H_{HT}}{H_{LT}}, \\
W_M &= \frac{W_{HT}}{H_{LT}}.
\end{aligned}
\tag{7}$$

If one of the calculated results is not integer, then it will be rounded to integer.

The sub-image which is covered by mask M should not overlap to each other. The mask of Gaussian uses the kernel of conventional Gaussian filter with the size $H_M \times W_M$, and different variances have been testified for the resizing works. The mask of mean average has the same size as C but uses the traditional mean average filter as its kernel.

The concepts of E and F are almost like C and D , respectively, but consider more about the blurred effect. The size of mask is designed to use a larger size to make those covered sub-images partially overlap. We have also tested multiple degrees of overlapping range, and the results will be shown in Chapter 3.

We have tested several resizing methods, and try to find out which method can generate templates which are close to the pattern of the origin VLP image.

2.3.2 Intensity Normalization

For the normalization of intensity, let NT be the normalized template after intensity normalization, LT be each character that is only normalized in size, the mean μ_{LT} and standard deviation σ_{LT} of each LT are calculated then. Let SLP be the

sub-image of LP that LT covers, and the mean μ_{SLP} and standard deviation σ_{SLP} are calculated too.

Then, the intensity values of each character template are normalized as follows:

$$NT(x, y) = (LT(x, y) - \mu_{LT}) \times \frac{\sigma_{SLP}}{\sigma_{LT}} + \mu_{SLP}. \quad (8)$$

2.4 Similarity Measurement

After the step of normalization is done, we use each normalized templates NT to determine the similarity with the character at each estimated character position. The L_1 distance [21] and Pearson's Correlation Coefficient (PCC) [22] are tested, both are conventional similarity measurement.

The L_1 distance is calculated by the following equation:

$$L_{1d} = \frac{1}{W_{NT} H_{NT}} \sum_{x=0}^{W_{NT}-1} \sum_{y=0}^{H_{NT}-1} |NT(x, y) - LP(x_p + x, y)|, \quad (9)$$

where x_p represents the start position on the x-axis of the sub-image of LP that NT covers. This measures the average difference between the template and the sub-image of LP that the template covers. However, the measurement cannot accurately tell the pattern difference. Fig. 7 shows an example. We can see that the first character "8" in LP has the characteristic that the top and bottom regions are black, but L_1 distances show that the most similar candidate is "H", which does not have this characteristic,

then "R", "P", ... , "8" is in the seventh rank.

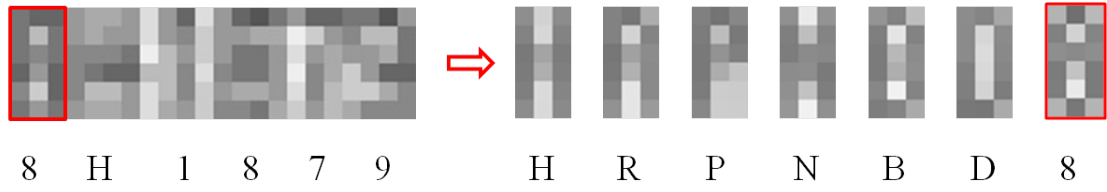


Fig. 7 The result of similarity measurement via L1 distance.

To solve this problem, the Pearson's Correlation Coefficient (PCC) is used and calculated as follows:

$$PCC = \frac{\sum_{x=0}^{W_{NT}-1} \sum_{y=0}^{H_{NT}-1} (NT(x, y) - \mu_{NT}) \cdot (LP(x_p + x, y) - \mu_{LP})}{\sqrt{\sum_{x=0}^{W_{NT}-1} \sum_{y=0}^{H_{NT}-1} (NT(x, y) - \mu_{NT})^2 \cdot \sum_{x=0}^{W_{NT}-1} \sum_{y=0}^{H_{NT}-1} (LP(x_p + x, y) - \mu_{LP})^2}}, \quad (10)$$

where μ_{NT} and μ_{LP} are the means of NT and the mean of the sub-image covered by NT , respectively. If the template and the character in the LP similar, the coefficient will be large. Fig. 8 shows that the correlation coefficient raises the similarity degree of "8" to the third rank.



Fig. 8 The result of similarity measurement via correlation coefficient.

2.5 Candidate Character Set Estimation

The candidate character set estimation is based on the result of single-character similarity measurement, the higher degree of similarity in each detected position shows that the character has a greater probability appearing in the corresponding position. The estimated character position may be biased, thus we take account of the estimation of neighbors in each detected position. Also, since we are dealing with the degraded VLP images, taking the top few closest characters instead of taking only one can avoid the recognition failure. Note that the digit region contains only digits, thus only digit patterns are considered for character recognition.

For multi-character matching, a cutoff threshold is used to take candidates which have higher similarity measures. The threshold is determined via averaging the similarity value of each character template in the corresponding position. And we set another threshold for candidate counts in single-character template matching. The threshold is set to 5 for digit region, and 18 for character region. Fig. 9 shows the estimated candidate positions and their corresponding candidates.

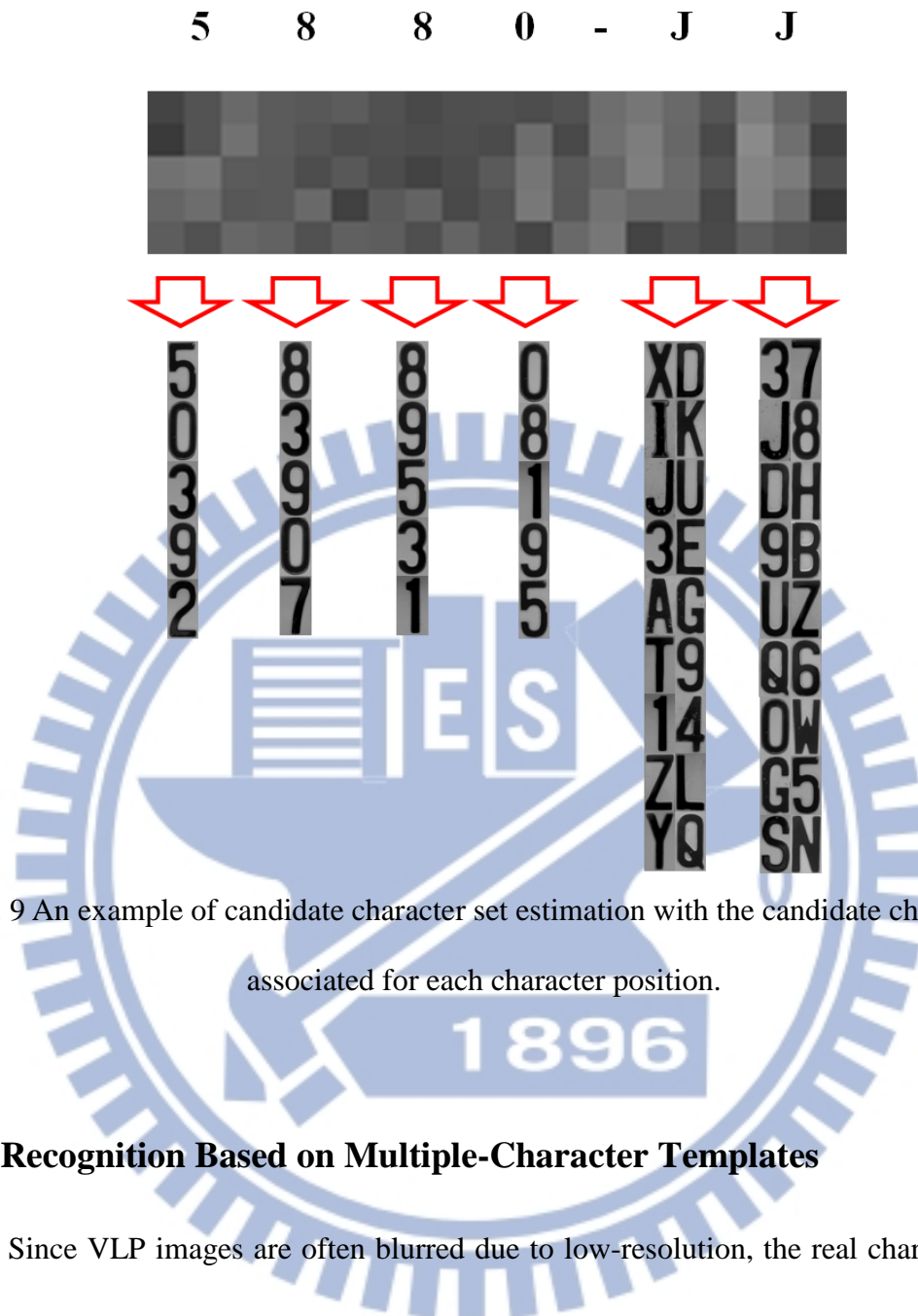


Fig. 9 An example of candidate character set estimation with the candidate characters associated for each character position.

2.6 Recognition Based on Multiple-Character Templates

Since VLP images are often blurred due to low-resolution, the real character by single-character template matching may not appear in the first rank. Therefore, after applying single-character template matching, we propose multiple-character template matching to refine the recognition result. Fig. 10 is the hierarchical structure of multiple-character templates with the hyphen at between the 2nd and 3rd characters. There are six characters and one hyphen on the VLP in Taiwan, so we need six nodes

that correspond to the six possible positions of characters at the bottom level. The second level from bottom shows all possible combinations of two characters, and so on. The hyphen should be concerned if it is needed.

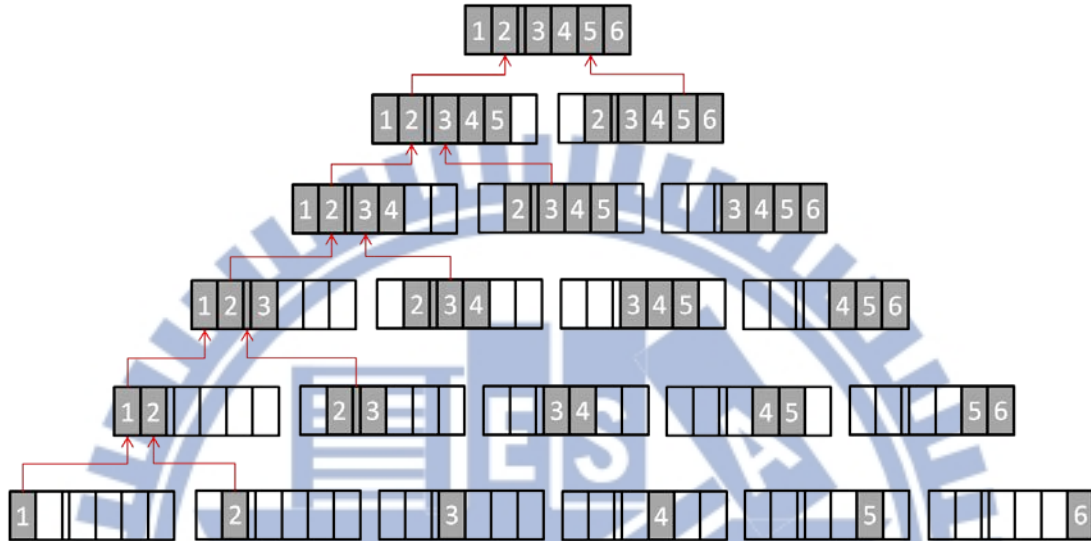


Fig. 10 The hierarchical structure of multiple-character template.

In Fig. 9, we have shown the candidate character sets of six positions via single-character template matching, each candidate character set is ordered according to the degree of similarity. The process of extending single-character template to two-character template is explained by this example.

The extending process needs to check where the hyphen should sit, and we then concern it in the concatenation of characters. The concatenation of characters is based on high-resolution character templates. We can list all possible two-character templates as follows. For the two-character templates of positions 1 and 2, since in the

single-character template matching, 5 candidate characters were identified at position 1, and 5 candidate characters were identified at position 2, we have 25 possible two-character templates at positions 1 and 2. For the two-character templates of positions 4 and 5, since in the single-character template matching, 5 candidate characters were detected at position 4, and 18 candidate characters were detected at position 5, we have 90 possible two-character templates at positions 4 and 5. The hyphen detection also told us that the hyphen sits between positions 4 and 5, so we have to insert the hyphen template at between positions 4 and 5 when the two-character template is used. Fig. 11 and Fig. 12 show the result of applying the two-character template matching. The normalization of the size and intensity are the same as the process of single-character template, and the remaining n-character template (n from three to six) matching uses the same methodology as that of two-character templates.

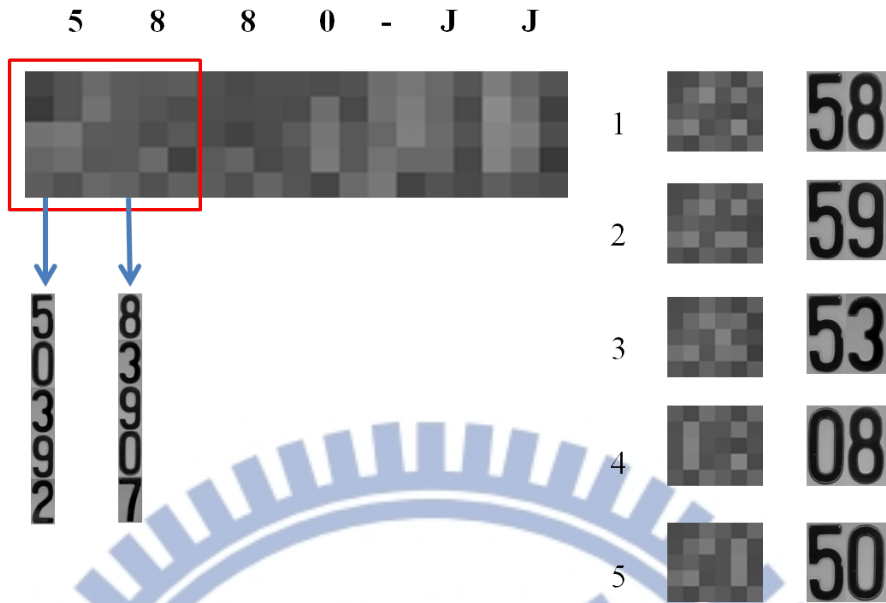


Fig. 11 The top survived 5 two-character templates after applying two-character template matching for positions 1 and 2.

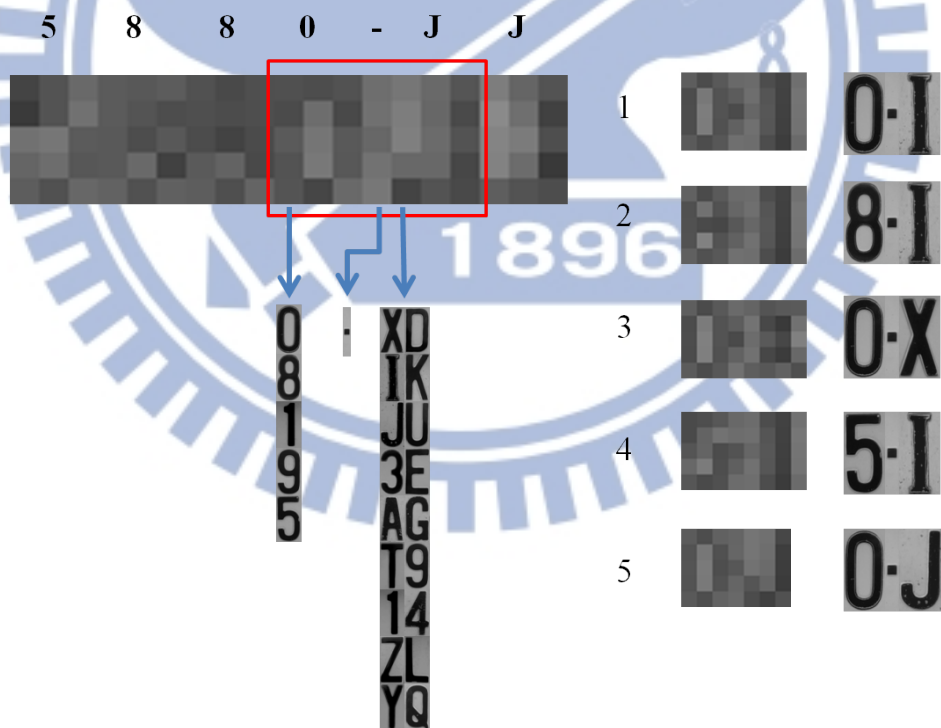


Fig. 12 The top survived 5 two-character templates after applying two-character template matching for positions 4 and 5.

CHAPTER 3

EXPERIMENTAL RESULTS

In this chapter, we present the experiment results of the proposed method. In the first part, we will discuss the experiments of six resizing methods, we will also compare the performance of similarity measurement by L1 distance with that by correlation coefficient. In the last part, we will present the experiment results of VLP recognition based on the resizing and similarity measuring methods we finally choose. The cropped VLP images we used as our test subjects are blurred, and the height of these images are at most 10 pixels.

3.1 Experiments of Resizing

In Chapter 2.3.1, 6 methods of resizing are mentioned, they are

- A. Bilinear interpolation,
- B. Bicubic interpolation,
- C. Mask of Gaussian,
- D. Mask of mean average,
- E. Mask of Gaussian with overlap,
- F. Mask of mean average with overlap.

The relation between Gaussian and mean average is that when the standard deviation (σ) of Gaussian becomes bigger, the weights of its kernel then become closer to the weights of mean average, in this case, the resizing results of using Gaussian and mean average are similar.

Table 2 shows the ranks of true characters applying the single-character template matching to 4 VLP images using bilinear, bicubic, Gaussian and mean average. σ of Gaussian we test are 3, 10 and 20. \times in table shows that the correct character is not in the candidate character set. The experiment results show that the bigger σ of Gaussian is, the higher the rank of the correct character is. The result also shows that mean average performs better than Gaussian and present the same performance as bicubic when using single-character template matching.

Table 2 The recognition results of using bilinear, bicubic, Gaussian and mean average for resizing.

Resizing method	Ranks of each position using single-character template matching																							
	VLP																							
	5	8	8	0	J	J	7	8	8	5	T	W	7	U	6	2	1	8	8	H	1	8	7	9
Bilinear	1	1	1	1	3	2	\times	1	1	1	5	2	1	4	2	1	1	3	12	6	1	\times	1	6
Bicubic	1	1	1	1	1	2	3	1	1	1	2	1	1	1	3	1	1	2	3	3	1	6	1	1
Gaussian ($\sigma = 3$)	1	1	2	1	3	2	3	1	1	1	2	1	1	3	2	1	1	2	3	4	1	\times	1	2
Gaussian ($\sigma = 10$)	1	1	1	1	3	2	5	1	1	2	2	1	1	1	3	1	1	2	3	3	1	6	1	2
Gaussian ($\sigma = 20$)	1	1	1	1	1	2	3	1	1	1	2	1	1	1	3	1	1	2	3	3	1	6	1	2
Mean average	1	1	1	1	1	2	3	1	1	1	2	1	1	1	3	1	1	2	3	3	1	6	1	1

However, we find out that when the blurring becomes more serious, the performance of multiple-character template matching via resizing methods mentioned above become weaker. To solve this problem, we try E and F to perform resizing, hope that the blurred effect caused by character overlapping can be solved. Table 3 and Table 4 show the recognition results of using different resizing methods, the overlap range is set to one quarter width of the mask. The experiment results show that we can get better performance of recognition if the overlap issue is concerned, and the resizing result of Gaussian with overlap and mean average with overlap are still similar when σ of Gaussian is big. So we decide to choose the mask of mean average with overlap as the solution of template size normalization.

Table 3 The recognition results of using different resizing methods on VLP “8H-1879”.

Resize method	σ	Ranks of each position using single-character template matching						Final rank
		8	H	1	8	7	9	
Bilinear	N/A	12	6	1	×	1	6	×
Bicubic	N/A	3	3	1	6	1	1	15
Mean average	N/A	3	3	1	6	1	1	×
	3	3	4	1	x	1	2	×
Gaussian	10	3	3	1	6	1	2	120
	20	3	3	1	6	1	3	106
Mean average with overlap	N/A	3	4	1	2	1	1	2
Gaussian with overlap	3	3	4	1	6	1	2	19
	10	3	5	1	5	1	1	4
	20	3	4	1	4	1	1	2

Table 4 The recognition results of using different resizing methods on VLP
"7885-TW".

Resize method	σ	Ranks of each position using single-character template matching						Final rank
		7	8	8	5	T	W	
Bilinear	N/A	×	1	1	1	5	2	×
Bicubic	N/A	3	1	1	1	2	1	49
Mean average	N/A	3	1	1	1	2	1	65
	3	5	1	1	2	2	1	54
Gaussian	10	3	1	1	1	2	1	64
	20	3	1	1	1	2	1	65
Mean average with overlap	N/A	2	1	1	1	3	1	3
Gaussian with overlap	3	2	1	1	1	5	1	16
	10	2	1	1	1	3	1	4
	20	2	1	1	1	3	1	3

Table 5 shows the experiment results using the resizing method, mask of mean average with overlap range of one-quarter width of mask on 15 VLP images. Both the similarity measurements mentioned in Chapter 2.4 are tested. As we expected, the experiment results of correlation coefficient has the greater performance than the measurement of L_1 distance.

Table 5 The recognition results using L_1 distance and correlation coefficient for 15 VLP images.

VLP	Rank	
	L_1 distance	Correlation Coefficient
5880-JJ	1	1
LW-4699	1	1
3870-KP	1	1
P7-2559	1	1
0457-FV	2	1
6293-HK	5	2
8H-1879	14	2
3729-N5	2	3
7885-TW	×	3
3R-5330	1	5
R3-1463	7	5
7U-6218	12	10
6411-VG	14	12
9826-TU	32	18
HF-1779	9	22

We also tested the overlap range from one-third, one quarter to one-fifth width of the resizing mask. Table 6 shows the recognition results of using three different overlap ranges on 15 VLP images. The experiment result shows that using one quarter width of mask as the overlap range have better results. Therefore, we decide to use one quarter width of the mask as the overlap range.

Table 6 The recognition results using different overlap ranges for 15 VLP images.

VLP	Rank		
	1/3 width of mask	1/4 width of mask	1/5 width of mask
5880-JJ	1	1	1
LW-4699	1	1	2
3870-KP	1	1	1
P7-2559	2	1	1
0457-FV	1	1	1
6293-HK	2	2	2
8H-1879	1	2	2
3729-N5	3	3	3
7885-TW	3	3	4
3R-5330	3	5	6
R3-1463	27	5	2
7U-6218	11	10	10
6411-VG	36	12	×
9826-TU	20	18	30
HF-1779	26	22	26

According to these experiments, we finally choose the mask of mean average with overlap as the resize method, and use correlation coefficient to perform similarity measurement. The overlap range is set to one-quarter width of mask.

3.2 Experiments of Proposed Method

50 cropped VLP images had been tested in the experiment. All of the resource images are blurred due to the poor resolution, and the height of cropped region is small. Fig. 14 and Fig. 15 show two results of VLP recognition via the proposed

method. In Fig. 14, the ground truth of the VLP is “5880-JJ”, and the experiment result shows that it is the top rank of recognition. In Fig. 15, the ground truth of VLP is “8H-1879”, which also has the second rank of the recognition result. The recognition results of 50 cropped VLP images are listed in Table 7, and the recognition result of the proposed method is showed in Table 8. With all 50 cropped VLP images, the proposed method has 70% accuracy to recognize the correct VLP within top 5 ranks, about 82% accuracy to refine the suspect range into top 10 ranks, and 94% accuracy to find the correct VLP of recognition within top 25 possible suspect VLP. The image of last two VLP without top 25 ranks is showed in Fig. 15. For VLP "2536-TX", the characteristic of each character is not clear due to the seriously blurred, especially the 6th character "X" . For VLP "M0-1860", the height is 4 pixels, which is not sufficient to present the characteristic of a single character.

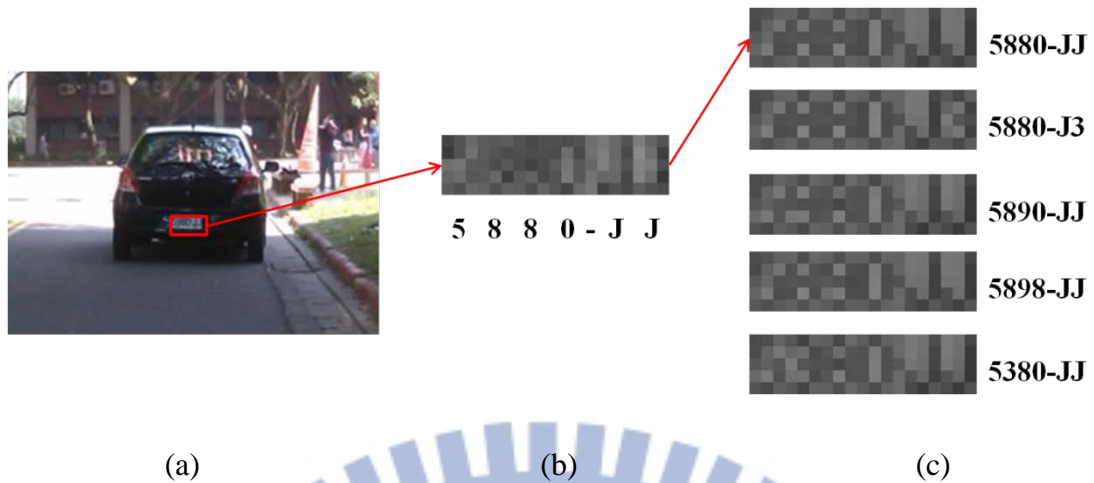


Fig. 13 Recognition result of VLP “5880-JJ”, (a) The low-resolution VLP image. (b) The cropped VLP image. (c) The top 5 ranks of recognition result: “5880-JJ”, “5880-J3”, “5890-JJ”, “5898-JJ” and “5380-JJ”.



Fig. 14 Recognition result of VLP “8H-1879”, (a) The low-resolution VLP image. (b) The cropped VLP image. (c) The top 5 ranks of recognition result: “BH-1879”, “8H-1879”, “RH-1879”, “BN-1879” and “BR-1879”.

Table 7 Recognition results of 50 cropped VLP images.

VLP	Rank	Size	VLP	Rank	Size	VLP	Rank	Size
5880-JJ	1	5*19	7U-3337	2	6*19	R3-1463	5	5*18
2209-EG	1	7*22	3E-5372	2	10*33	3761-YV	6	6*22
3870-KP	1	6*22	0077-HR	2	6*21	2136-ZD(2)	8	5*18
P7-2559	1	6*20	6293-HK	2	6*22	W2-3000	9	6*22
0457-FV	1	7*22	2301-MY	2	6*19	1531-TV	9	5*18
9392-XL	1	7*26	8H-1879	2	6*22	8757-YW(2)	10	5*18
9153-P2	1	8*27	3729-N5	3	6*22	7U-6218	10	7*25
R3-0179	1	8*29	8757-YW(1)	3	7*22	6411-VG	12	5*18
7E-8971	1	7*23	7885-TW	3	8*24	5961-S2	15	6*20
9521-JU	1	9*31	5P-9871	3	7*21	DP-3719(1)	16	6*17
LW-4699	1	6*19	0388-FH	3	6*20	9826-TU(2)	18	6*19
DM-1515	1	7*26	3528-M8	3	7*23	HF-1779	22	5*19
5827-FL	1	6*25	2136-ZD(1)	3	6*21	DP-3719(2)	25	5*18
9538-EH	1	6*23	AV-5590	4	7*24	8387-HL	82	7*21
JV-1392	1	6*18	9467-N3	5	8*31	2536-TX	656	5*18
9826-TU(1)	1	5*20	HF-1779(2)	5	6*21	M0-1860	×	4*18
0053-KW	1	5*18	3R-5330	5	5*19			

Table 8 The recognition result of the proposed method.

Rank	1~5	6~10	11~25	26~
VLP count	35	6	6	3
Percentage	70%	12%	12%	6%



2 5 3 6 - T X



M 0 - 1 8 6 0

Fig. 15 The images of VLP "2536-TX" and "M0-1860".



CHAPTER 4

CONCLUSIONS AND FUTURE WORK

In this thesis, a recognition method for a low-resolution VLP image is proposed.

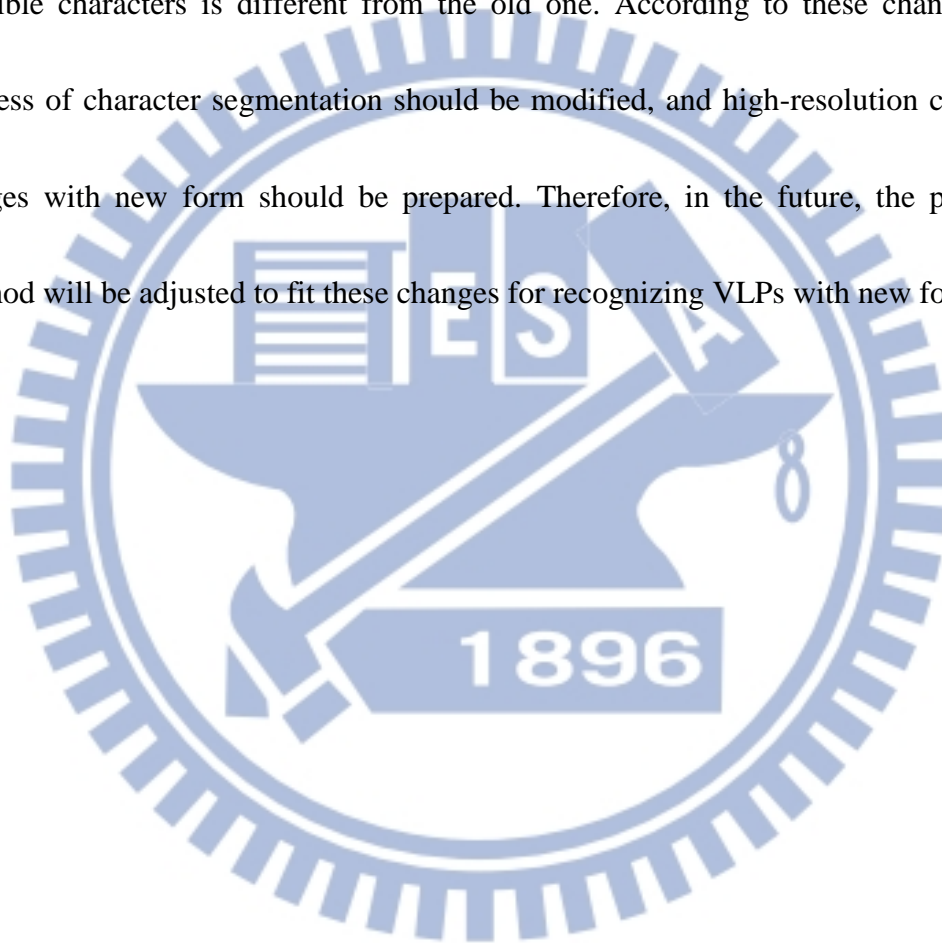
This method can treat VLP images with pretty small size. The proposed method only need a single VLP image to perform recognition process, and the extending of single-character template to multiple-character template can refine the recognition results to a small range.

In this method, at first, the hyphen detection and character position estimation are performed on the cropped low-resolution VLP image to locate the possible positions of characters and hyphen. Second, we use single-character template matching to estimate the candidate characters of each corresponding position. At last, we extend the single-character template to multiple-character template, and use multiple-character template matching to refine the results of recognition.

The experiment of results show that this method is quite efficient to recognize VLP images with low resolution, these results can be helpful for locating a suspect vehicle on a low-resolution image in the field of crime investigation.

The input images we use in this research are not strongly affected by illumination variation, weather and prospective distortion. These affections may

influence the efficacy of recognition. In the future, we want to take these situations into account to reduce failure recognitions caused by these affections. Besides, the form of VLP in Taiwan is updated since December 17, 2012. The VLP of a light vehicle with new form have 7 characters and a hyphen. Also, the license plate font of possible characters is different from the old one. According to these changes, the process of character segmentation should be modified, and high-resolution character images with new form should be prepared. Therefore, in the future, the proposed method will be adjusted to fit these changes for recognizing VLPs with new form.



REFERENCES

- [1] C.-N. E. Anagnostopoulos, I. E. Anagnostopoulos, I. D. Psorulas, V. Loumos, and E. Kayafas, "License plate recognition from still images and video sequences: a survey," *IEEE Transactions on Intelligent Transportation Systems*, vol. 9, no. 3, pp. 377-391, Sep. 2008.
- [2] H. L. Bai, and C. P. Liu, "A hybrid license plate extraction method based on edge statistics and morphology," in *Proc. IEEE International Conference on Pattern Recognition, ICPR'04*, vol. 2, Aug. 2004, pp. 831-834.
- [3] H. H. Wu, H. H. Chen, R. J. Wu, and D. F. Shen, "License plate extraction in low resolution video," in *Proc. IEEE International Conference on Pattern Recognition, ICPR'2006*, vol. 1, Hong Kong, Aug. 2003, pp. 824-827.
- [4] Y. Zhang, and C. Zhang, "A new algorithm for character segmentation of license plate," in *Proc. IEEE Intelligent Vehicles Symposium, IV'2003*, Columbus, OH, USA, 9-11 June 2003, pp. 106-109.
- [5] S. Nomura, K. Yamanaka, O. Katai, H. Kawakami, and T. Shiose, "A novel adaptive morphological approach for degraded character image segmentation," *Pattern Recognition*, vol. 38, no. 11, pp. 1961-1975, 2005.
- [6] D. Llorens, A. Marzal, V. Palazón, and J. M. Vilar, "Car license plates extraction

and recognition based on connected components analysis and HMM decoding," in *Proc. Pattern Recognition and Image Analysis, IbPRIA'2005*, LNCS vol. 3522, Estoril, Portugal, 7-9 June 2005, pp. 571-578, Springer Berlin Heidelberg.

- [7] K. K. Kim, K. I. Kim, J. B. Kim, and H. J. Kim, "Learning-based approach for license plate recognition," in *Proc. IEEE Signal Processing Society Workshop, Neural Networks for Signal Processing X*, vol. 2, Sydney, NSW, AUS, Dec. 2000, pp. 614-623.
- [8] S. L. Chang, L. S. Chen, Y. C. Chung, and S. W. Chen, "Automatic license plate recognition," *IEEE Transactions on Intelligent Transportation Systems*, vol. 5, no. 1, pp. 42-53, Mar. 2004.
- [9] Y. P. Huang, S. Y. Lai, and W. P. Chuang, "A template-based model for license plate recognition," in *Proc. IEEE International Conference on Networking, Sensing and Control, ICNSC'04*, vol. 2, Taipei, Taiwan, Mar. 2004, pp. 737-742.
- [10] C. Wu, L. C. On, C. H. Weng, T. S. Kuan, and K. Ng, "A Macao license plate recognition system," in *Proc. IEEE International Conference on Machine Learning and Cybernetics, ICMLC'05*, vol. 7, Cuangzhou, 18-21 Aug. 2005, pp. 4506-4510.
- [11] N. Bellas, S. M. Chai, M. Dwyer, and D. Linzmeier, "FPGA implementation of a license plate recognition SoC using automatically generated streaming

- accelerators," in *Proc. IEEE International Parallel and Distributed Processing Symposium, IPDPS'06*, Rhodes Island, Greece, Apr. 2006, pp. 8-pp.
- [12] J. Barroso, E. L. Dagless, A. Rafael, and J. Bulas-Cruz, "Number plate reading using computer vision," in *Proc. IEEE International Symposium on Industrial Electronics, ISIE'97*, vol. 3, Guimaraes, Portugal, July 1997, pp. 761-766.
- [13] P. Comelli, P. Ferragina, M. N. Granieri, and F. Stabile, "Optical recognition of motor vehicle license plates," *IEEE Transactions on Vehicular Technology*, vol. 44, no. 4, pp. 790-799, Nov. 1995.
- [14] S. C. Lin, and C. T. Chen, "Reconstructing vehicle license plate image from low resolution images using nonuniform interpolation method," *International Journal of Image Processing (IJIP)*, vol. 1, no. 2, pp. 21-28, 2008.
- [15] K. V. Suresh, G. M. Kumar, and A. N. Rajagopalan, "Superresolution of license plates in real traffic videos," *IEEE Transactions on Intelligent Transportation Systems*, vol. 8, no. 2, pp. 321-331, June 2007.
- [16] S. Rajaram, M. D. Gupta, N. Petrovic, and T. S. Huang, "Learning-based nonparametric image super-resolution," in *EURASIP Journal on Advances in Signal Processing*, vol. 2006, pp.1-11, Jan. 2006.
- [17] Y. Tian, K. H. Yap, and Y. He, "Vehicle license plate super-resolution using soft learning prior," *Multimedia Tools and Applications*, vol. 60, no. 3, pp. 519-535,

Oct. 2012.

- [18] C. C. Chen, and J. W. Hsieh, "License Plate Recognition from Low-Quality Videos," in *IAPR Conference on Machine Vision Applications, MVA'2007*, Tokyo, JAPAN, May 2007.
- [19] K. Nakao, K. Sugimoto, M. Saitoh, and T. Okazaki, "The development of a license plate number recognition system incorporating low-resolution cameras," *Mitsubishi Heavy Industries Technical Review*, vol. 45, no. 3, Sep. 2008
- [20] P. L. Hsieh, Y. M. Liang, and H. Y. M. Liao, "Recognition of Blurred License Plate Images," in *Proc. IEEE International Workshop, Information Forensics and Security, WIFS'2010*, Seattle, WA, USA, 12-15 Dec.2010, pp. 1-6.
- [21] E. Krause, *Taxicab geometry: An adventure in non-Euclidean geometry*, DoverPublications, 1987
- [22] R. Lee, J., and W. A. Nicewander, "Thirteen ways to look at the correlation coefficient," *The American Statistician*, vol. 42, no. 1, pp. 59-66, 1988.